NASA TECHNICAL MEMORANDUM

NASA TM X-72625

NASA TM X-72625

MICROWAVE INTERFEROMETRY TECHNIQUE FOR OBTAINING GAS INTERFACE VELOCITY MEASUREMENTS IN AN EXPANSION TUBE FACILITY

By Charles C. Laney, Jr.

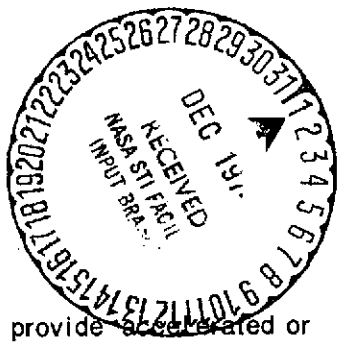

NATIONAL AERONAUTICS AND SPACE ADMINISTRATION

LANGLEY RESEARCH CENTER, HAMPTON, VIRGINIA 23665

1. Report No.	2. Government Accession No.	3. Recipient's Catalog No.
TM X-72625		

4. Title and Subtitle	5. Report Date
Microwave Interferometry Technique for Obtaining Gas Interface Velocity Measurements in an Expansion Tube Facility	Nov. 13, 1974
	6. Performing Organization Code
7. Author(s)	8. Performing Organization Report No.
Charles C. Laney, Jr.	
9. Performing Organization Name and Address	10. Work Unit No.
NASA Langley Research Center Hampton, VA 23665	506-26-20-04
	11. Contract or Grant No.
	13. Type of Report and Period Covered
12. Sponsoring Agency Name and Address	Technical Memorandum
National Aeronautics and Space Administration Washington, DC 20546	14. Sponsoring Agency Code

15. Supplementary Notes

16. Abstract

This paper describes a microwave interferometer technique to determine the front interface velocity of a high enthalpy gas flow in an expansion tube facility with sufficient resolution to approximate instantaneous measurements. The system is designed to excite a standing-wave in the expansion tube and to measure the shift in this standing wave as it is moved by the test gas front. Data, in the form of a varying sinusoidal signal, is recorded on a high-speed drum camera-oscilloscope combination. Measurements of average and incremental velocities in excess of 6,000 meters per second have been made.

17. Key Words (Suggested by Author(s)) (STAR category underlined)

Instrumentation, microwave interferometry, shock tube velocity measurements

18. Distribution Statement

Unclassified - Unlimited

19. Security Classif. (of this report)	20. Security Classif. (of this page)	21. No. of Pages	22. Price*
Unclassified	Unclassified	29	$3.75

*Available from { The National Technical Information Service, Springfield, Virginia 22151
STIF/NASA Scientific and Technical Information Facility, P.O. Box 33, College Park, MD 20740

SUMMARY

An accurate knowledge of the instantaneous test gas velocity and acceleration is of primary importance in shock and expansion tube work. However such knowledge is difficult to obtain due to the absence of a continuous velocity measurement. This paper describes the use of an economical microwave interferometer technique to determine the front interface velocity of a high enthalpy gas flow in a 3.75 inch diameter 70 foot expansion tube with sufficient resolution to approximate instantaneous measurements. The system is designed to excite a standing-wave in the expansion tube and to measure the shift in this standing wave as it is moved by the test gas front. Data, in the form of a varying sinusoidal signal, is recorded on a high-speed drum camera-oscilloscope combination. Measurements of average and incremental velocities in excess of 20,000 feet per second have been made. Average velocity measurements were made to an accuracy of 1.0%; incremental velocities over 5.0 inch distances were made to an accuracy of 3.0%.

INTRODUCTION

Velocity measurements of shock waves and test gas interfaces are made at the LRC Reentry Physics 4-Inch High-Pressure Shock Tube (used as an expansion tube) using ionization detectors, photo-detectors, and pressure detectors. All of these systems yield the average velocity between two stations a fixed distance apart. As the shock wave or test gas interface passes a station the phenomena detected (ionization, light, or pressure)

triggers a pulse which starts an electronic time interval meter and at the next station another pulse is generated which stops the time interval meter. The average velocity is then calculated knowing the distance between stations and time between pulses. The accuracy of these systems is completely dependent on the ability to trigger at the same corresponding points on the detection signals since the electronic circuitry can respond in .1 microsecond. Precursor radiation can prematurely trigger ionization and photodetection systems but only affects the accuracy when there are small distances between stations.

In order to study the gas acceleration and velocity time histories in the shock tube, it was considered sufficient that the velocity be measured in distance increments of about a half of foot. In a 70 foot shock tube this would amount to 140 measuring stations with a prohibitive amount of associated electronic equipment. This report will describe a microwave interferometer technique which has the same capability of measuring incremental and average velocities as other techniques, and as accurately, without the need of multiple measuring stations. The instrumentation aspects and readout methods used in attaining the velocity profile will be discussed and the microwave technique will be compared with ionization, pressure, and photodetection methods.

SYMBOLS

c	velocity of light, 2.99776×10^8 m/sec
d	plasma slab thickness, cm
f_c	mode cutoff frequency, cycles/sec
f_p	plasma frequency, cycles/sec
Ne	electron concentration, electrons/cm^3
r	radius, cm
TE_{11}	fundamental transverse electric mode
TM_{01}	fundamental transverse magnetic mode
$\bar{v}$	average velocity, feet/sec
ΔX	abscissa scale factor
ΔY	ordinate scale factor
Γ_p	power reflection coefficient
Γ_v	voltage reflection coefficient
θ	angle of time versus distance curve, degrees
θ_{Γ_v}	phase angle of voltage reflection coefficient, degrees
λ	free-space wavelength, cm
λ_c	mode cutoff wavelength, cm
λ_g	wavelength inside guide, cm
ν	collision frequency, collisions/sec
ρ	density, gram/cm^3
ρ_o	STP density, 1.28823×10^{-3} grams/cm^3

DESCRIPTION OF APPARATUS

The principle component of the interferometer system is the hybrid or magic tee.[1] Characteristics of the hybrid are: If the two side branches I and II have the same length and are terminated identically, then power delivered to the system at branch S divides at the junction and flows equally to I and II, with very little output (over 40DB down) being obtained at branch P. If power is delivered to the system at branch S and the terminations at branches I and II are not identical, then there will be an output at branch P proportional to the difference between the waves reflected at branches I and II. It is the function of the interferometer system to introduce microwave energy into the expansion tube, excite a standing wave in the tube due to the reflection of the termination, and then detect the movement of this standing wave due to the movement of the termination as a function of time.[2]

The tuning stub, variable attenuator, and adjustable short in branch I (Figure 1) allows complete impedance selection for this branch. Branch II consists of 25 feet of RG-9B/U cable which runs to a 3/16 inch diameter stainless steel antenna, that protrudes about 3.5 inches into the 3.75 inch diameter tube. The signal is detected at branch P using a 1N23C diode and is fed to an oscilloscope with millivolt sensitivity and a short duration phosphor. Data is recorded on a high speed drum camera which has a writing speed capability of 4800 inches per second. The camera has a speed monitor output which supplies a sine wave, four cycles per revolution, which is fed to an EPUT (events per unit time)

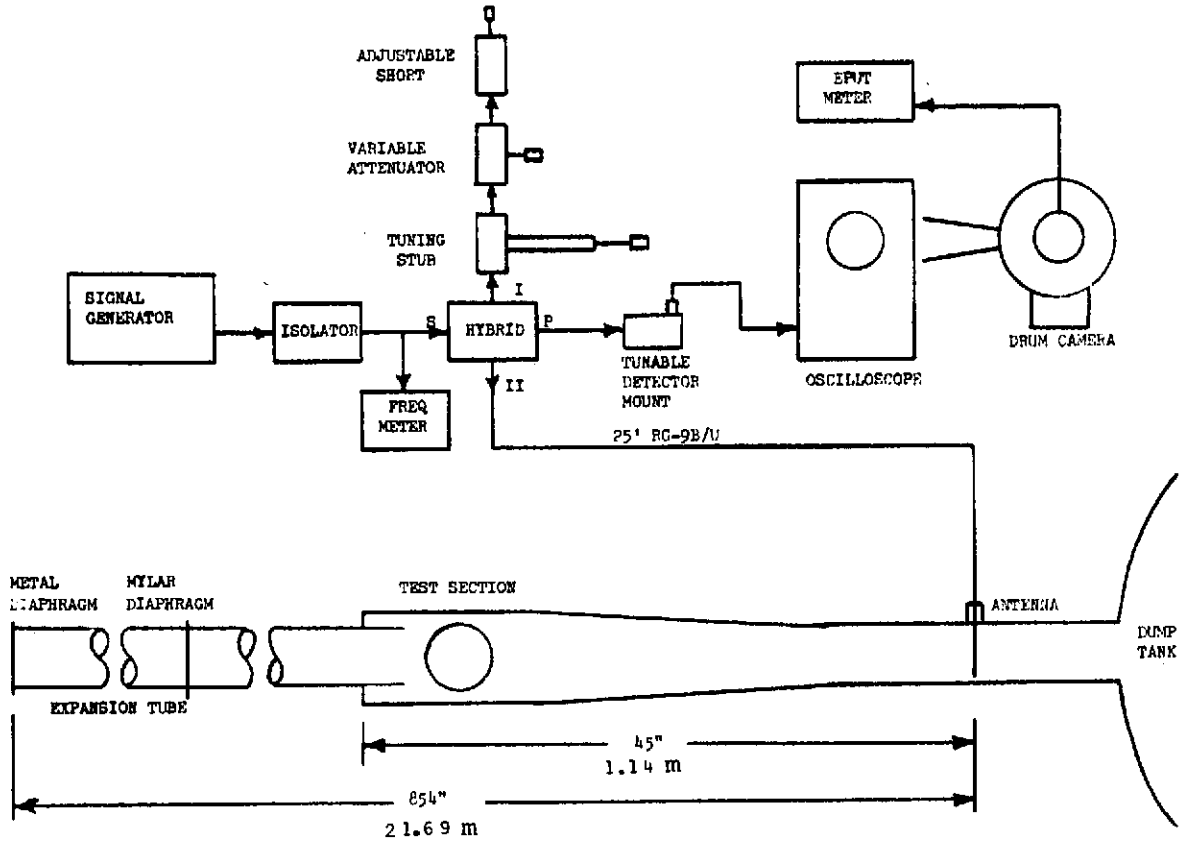

FIGURE 1. MICROWAVE INTERFEROMETER AND EXPANSION TUBE COMPONENTS

meter set to count over 1 second intervals. One hundred microsecond timing markers from the EPUT meter can be put on the other beam of the oscilloscope but little gain in accuracy would result.

PROCEDURE

The signal generator is adjusted to put out 1 milliwatt at 2.1758 kmc. This frequency was chosen arbitrarily between the limits; any frequency which is higher than cutoff frequency for the fundamental mode (TE_{11}) in the expansion tube but lower than the cutoff frequency for the next higher mode (TM_{01}) would be acceptable.[3] Cutoff wavelength for a circular

waveguide and the fundamental mode ($\lambda_{c_{TE_{11}}}$) is roughly 3.412 times the radius in centimeters so with 3.75 inch diameter guide (expansion tube).

$$\lambda_{c_{TE_{11}}} = 3.412r = 3.412(2.54)(3.75/2) = 16.28 \text{ cm}$$

$$f_{c_{TE_{11}}} = \frac{c}{\lambda} = 1.842 \text{ kmc}$$

Cutoff wavelength for the next higher mode ($\lambda_{c_{TM_{01}}}$) is 2.61 times the radius in centimeters or

$$\lambda_{c_{TM_{01}}} = 2.61r = 12.24 \text{ cm}$$

$$f_{c_{TM_{01}}} = 2.415 \text{ kmc}$$

Therefore any frequency between 1.842 and 2.415 kmc will excite the fundamental mode in the expansion tube. Operation at higher frequencies would be acceptable since the method used in exciting the wave in the tube is much more favorable for the TE_{11} mode.

With the generator set on 2.1758 kmc, the tuning stub, variable attenuator, and adjustable short are set until a maximum negative DC voltage is observed on the oscilloscope. This represents the greatest mismatch in the impedance of branch I as compared to branch II and it was found that the signal generated under this condition is larger than the signal generated when branches I and II are balanced. The antenna is placed as shown in Figure 1 to excite the fundamental mode in the expansion tube. Since it was desired that the microwave system not interfere with the function of the expansion tube, no reflecting plate could be located at a quarter of a wavelength from the antenna and at least half the energy introduced at the antenna is lost in the dump-tank.

When microwave energy is introduced into the expansion tube as described above, a standing wave is set up in the tube (Figure 2). The

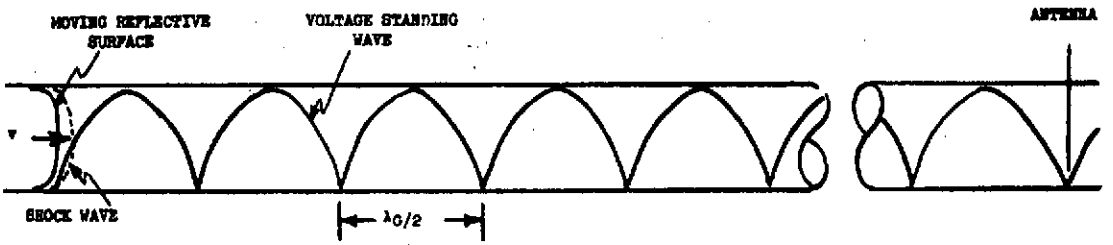

FIGURE 2. STANDING WAVE IN EXPANSION TUBE.

distance between two voltage maximums or minimums is half of the guide wavelength, λ_g. λ_g is defined as [4]

$$\lambda_g = \frac{\lambda}{\sqrt{1 - \left(\frac{\lambda}{\lambda_c}\right)^2}}$$

where

λ free space wavelength

λ_c cutoff wavelength = 3.412r (cm)

If the diameter of the tube was uniform and known to a thousandth of an inch, then the wavelength in guide could be calculated very accurately. The inside of the tube was measured and found to vary between 3.750 and 3.757 inches in diameter, which yielded a $\lambda_g/2$ or 5.113 inches and 5.089 inches respectively. Although these two figures are within 1/2% of each other, the cumulative error would result in a 3 inch uncertainty in the position of the reflective surface when it reaches the transition from the expansion tube to the test section. To illustrate, assume the velocity

record will be obtained between station 3 and transition from the expansion tube to the test section. This is a distance of 665.56 inches (Figure 3). Since a cycle of record is generated everytime the reflective

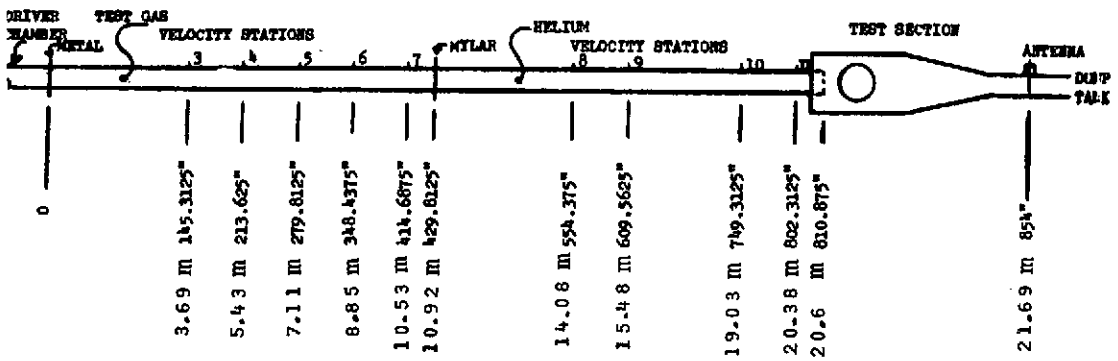

FIGURE 3. DIAPHRAGM AND STATION LOCATION OF THE EXPANSION TUBE.

surface moves a $\lambda_g/2$, this would amount to 130.17 cycles for the 5.113 $\lambda_g/2$ and 130.77 cycles for the 5.089 $\lambda_g/2$. The difference would be about 0.6 cycle or about 3 inches. It was therefore decided to calibrate the expansion tube by measuring the number of cycles between station 3 and the transition.

To calibrate the expansion tube a 6 inch long 3-5/8 inch diameter piece of wood with a 1/4 thick brass front plate (representing a perfect reflector) was pulled through the expansion tube and the total number of cycles between station 3 and the transition was measured. Figure 4

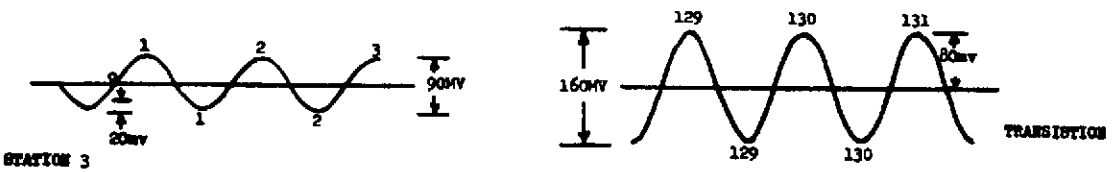

45 SIN WT = -25

WT = -33.75°

33.75/360 = .09375 CYCLE

TOTAL NUMBER CYCLES (STATION 3 TO TRANSITION) = .09375 + 130 + .5
= 130.59375 CYCLES

FIGURE 4. DETERMINATION OF AVERAGE $\lambda_g/2$ FOR THE EXPANSION TUBE.

shows the voltage on the oscilloscope as a function of reflective surface position. The total number of cycles was found to be 130.6. Therefore the average $\lambda_g/2$ was determined to be (665.56/130.6). Throughout this report generator frequency will be fixed at 2.1758 kmc and $\lambda_g/2$ will be assigned the value of (665.56/130.6) inches.

With the position of the reflective surface in the expansion tube known as a function of the cycle maximums, the system is ready for a run. The oscilloscope drum camera is set to run at about 130 revolutions per second and the EPUT meter is used to measure the film speed during the run. An ionization probe located at station 3 is used to trigger the oscilloscope sweep.

The expansion tube is set in action by bursting the metal diaphragm (Figure 3). When this diaphragm ruptures, a shock wave travels through the test gas, (which is usually air) heating and accelerating it. This shock progresses through the test gas, strikes the mylar diaphragm separating the test gas from the accelerating gas (which is usually helium), breaks this diaphragm and a new shock wave propagates into the accelerating gas. At the same time, an upstream expansion wave is formed, progressing back into the test gas, but since the flow is supersonic, the expansion wave is washed downstream. This expansion accelerates the test gas from the velocity resulting from the shock wave passing through it to a higher velocity, and at the same time causes a decrease in temperature and pressure. Consequently we now have gas at a very high velocity which has been accelerated by two processes, one a shock and one an expansion. The ambient conditions are now at a low temperature and pressure because the expansion has reduced the temperature and pressure from the high values created in the test gas by the passage of the shock wave.[5]

From the above paragraph the important thing to remember is that when the metal diaphragm ruptures, a shock wave, followed by the test gas, progresses toward the mylar diaphragm at some velocity. When the mylar diaphragm ruptures a new shock wave at a higher velocity is generated again followed by the test gas. When the shock wave passes station 3, the oscilloscope sweep will be triggered and a sine wave will be generated by the movement of the reflective surface (the front interface of the gas flow). By measuring the time of occurance of the maximums on the drum camera record, the time position and hence velocity can be determined.

PRECISION

The precision of the velocity measurement depends primarily on the accuracy to which the distance between maximums is known and on the accuracy with which the time between these maximums can be determined.

The distance between maximums was determined by calibrating the tube as described in the Procedure. An average distance was determined since the diameter of tube varied over about .007 inch. In determining the velocity over a one cycle increment of record, with this one cycle representing a movement of the reflective surface through a portion of the tube of minimum diameter, the error in the distance measurement would be less than .4%.

The generator frequency is the other parameter which effects the accuracy of $\lambda_g/2$. After about an hour warm-up time the generator short term frequency drift is very small. The generator frequency is determined by using a frequency meter as shown in Figure 1 and the maximum error in using this device could be 1.4 mc (1 division on the

dial). Operating at 2.1758 kmc this amounts to a maximum error in frequency of .07%.

The time between maximums is obtained from the drum camera film record. There are three parameters effecting the accuracy of this measurement. They are film speed, film resolution, and film length stability. The film speed measurement is made using the EPUT meter. The drum camera puts out a sine wave, 4 cycles per revolution which (at 130 revolutions per second) would amount to 520 events per second the EPUT meter would have to count. Since EPUT meter is accurate to $\pm$ 1 count, the film speed can be determined to within 0.2%. Film resolution or the ability to resolve distances on the film can be made to about 0.0025 inch and at 130 revolutions per second film speed, this amounts to about 0.6 microsecond resolution. Film length stability is very good. Under the worst environmental and processing conditions, maximum length variations are within $\pm$ 1/2%.

Therefore considering all sources of errors, the accuracy of the average velocity measurement obtained using this technique should be within at least 1%. Of course, in measuring incremental velocities whose time between maximums on the film is 20 microseconds, (With 0.6 microsecond resolution) a 3% accuracy is the best that can be obtained.

RESULTS

A typical data record is shown in figure 5. (It was cut in 3 sections for presentation in this report). This data represents run number 1850 at the shock tube facility. The prerun conditions were:

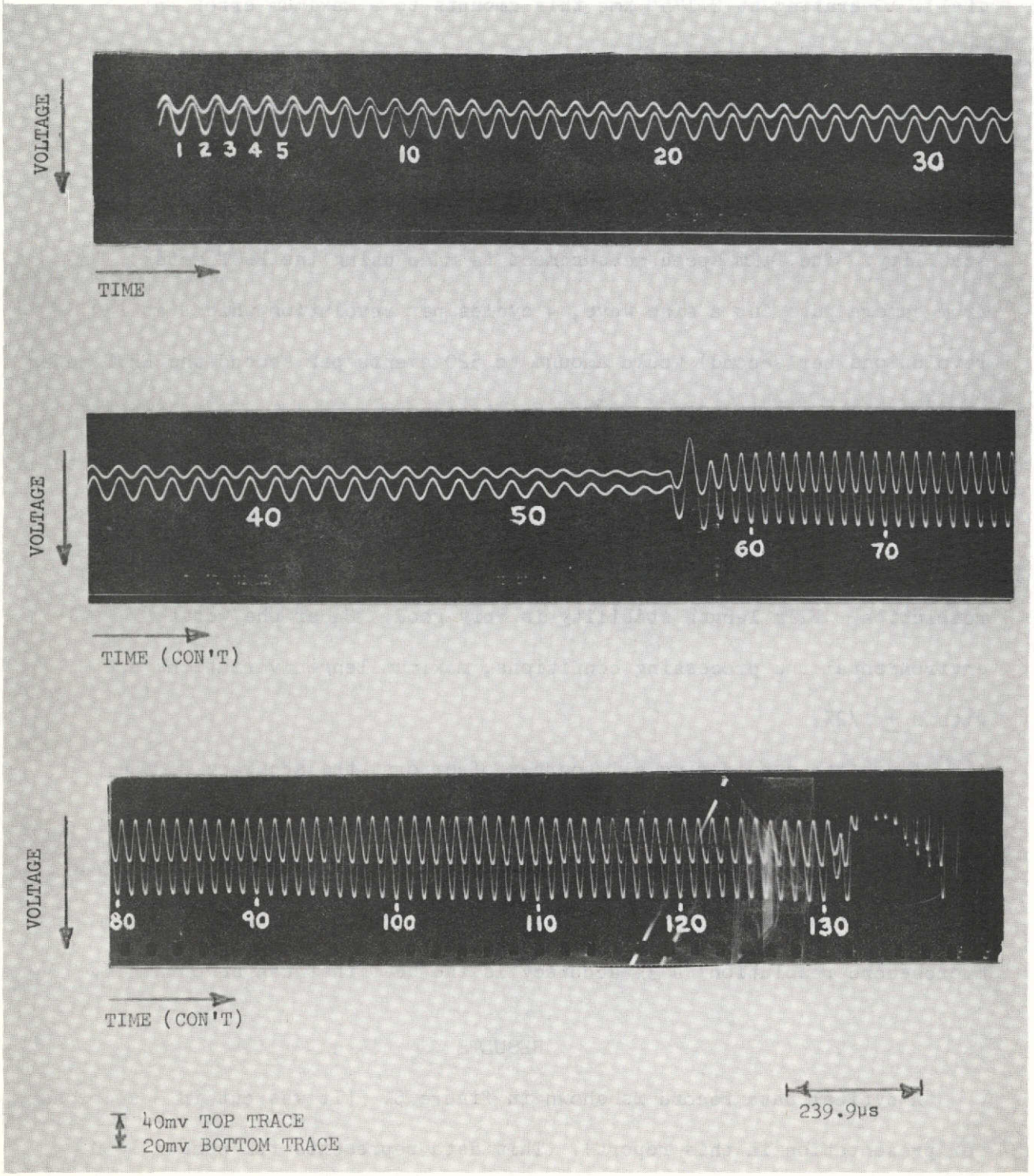

FIGURE 5. TYPICAL DATA RECORD

(1) Pressure of test gas (between metal and mylar diaphragms) - Air at 22 mm Hg

(2) Pressure of expansion tube (mylar diaphragm to test section) - Helium at .470 mm Hg

(3) Temperature of test gas - 72°F

(4) Mylar diaphragm thickness - 1/4 mil

Data reduction of the film record yields the distance between maximums and position synchronization. The distance between maximums is measured using a 6 power comparator and is accurate to 0.0025 inch. Table 2 gives a tabulation of distances. To convert this distance into a time between peaks the film speed must be calculated.

Writing speed = Film circumference x revolutions per second

Writing speed = π(drum diameter - 2x film thickness) rev per second

$= \pi[10.708-2(.0061)]\ 124.25$

$= 4166.64$ in/sec (239.9 μs/in)

Table 2 lists the results of the conversion of distances to times between peaks.

To determine the time of the occurance of peak number 1 with respect to the reflective surface passage of station 3, the following procedure is used. The distance between station 3 and the mylar diaphragm amounts to 55.8 cycles (distance between 3 and mylar $+ \lambda_g/2$). However, using the mylar diaphragm as a reference point on the run record (Note sharp discontinuity between peaks 55 and 56 in Figure 5), the number of cycles of record from peak 1 to the mylar diaphragm (Figure 5) is 54.5 Therefore 1.3 cycles should precede peak 1 (.8 cycle is recorded). The half cycle

of record "missing" amounts to about 20 microseconds. This may be interpreted to mean that 20 microseconds after the reflective surface passes station 3, the scope sweep begins (the significance of this will be discussed later). The time from station 3 to peak 1 is then found to be 55.9 microseconds with the position of peak 1, 1.26 cycle from station 3. The time of occurance of the subsequent peaks are listed under cumulative time in table 2. Each of these peaks represents reflective surface movement of $\lambda_g/2$ or (665.56/130.6) inches

As mentioned before, the mylar diaphragm position is assumed to be between peaks 55 and 56 (note sharp transition in figure 5). This point acts as position synchronization for distance measurements. The film record should contain 55.8 cycles before this point and 74.8 cycles after since the total length of record from station 3 to the transition at the test section is 130.6 cycles.

Figure 6 is a plot of the time the reflective surface passes a position versus this position. The result is two faired in straight lines, the slope of which in the first case reciprocal of the average velocity in the tube before mylar diaphragm rupture and the other reciprocal of the average velocity after rupture. The angle of the first line is 42°.

Therefore, for the average velocity before the diaphragm

$$\text{Slope} = \frac{1}{\bar{v}} = \tan\theta$$

$$\bar{v} = \text{cotan}\,\theta\left(\frac{\Delta x}{\Delta y}\right) = \text{cotan}\,\theta\left(\frac{1.02\text{ in}}{10\ \mu\text{s}}\right) = .102\ \text{cotan}\,\theta\ \frac{\text{in}}{\mu\text{s}}$$

$$= 9{,}444.4 \text{ feet/sec}$$

For the average velocity after the diaphragm, where = 25.8°

$$\bar{v} = 17{,}598.3 \text{ ft/sec}$$

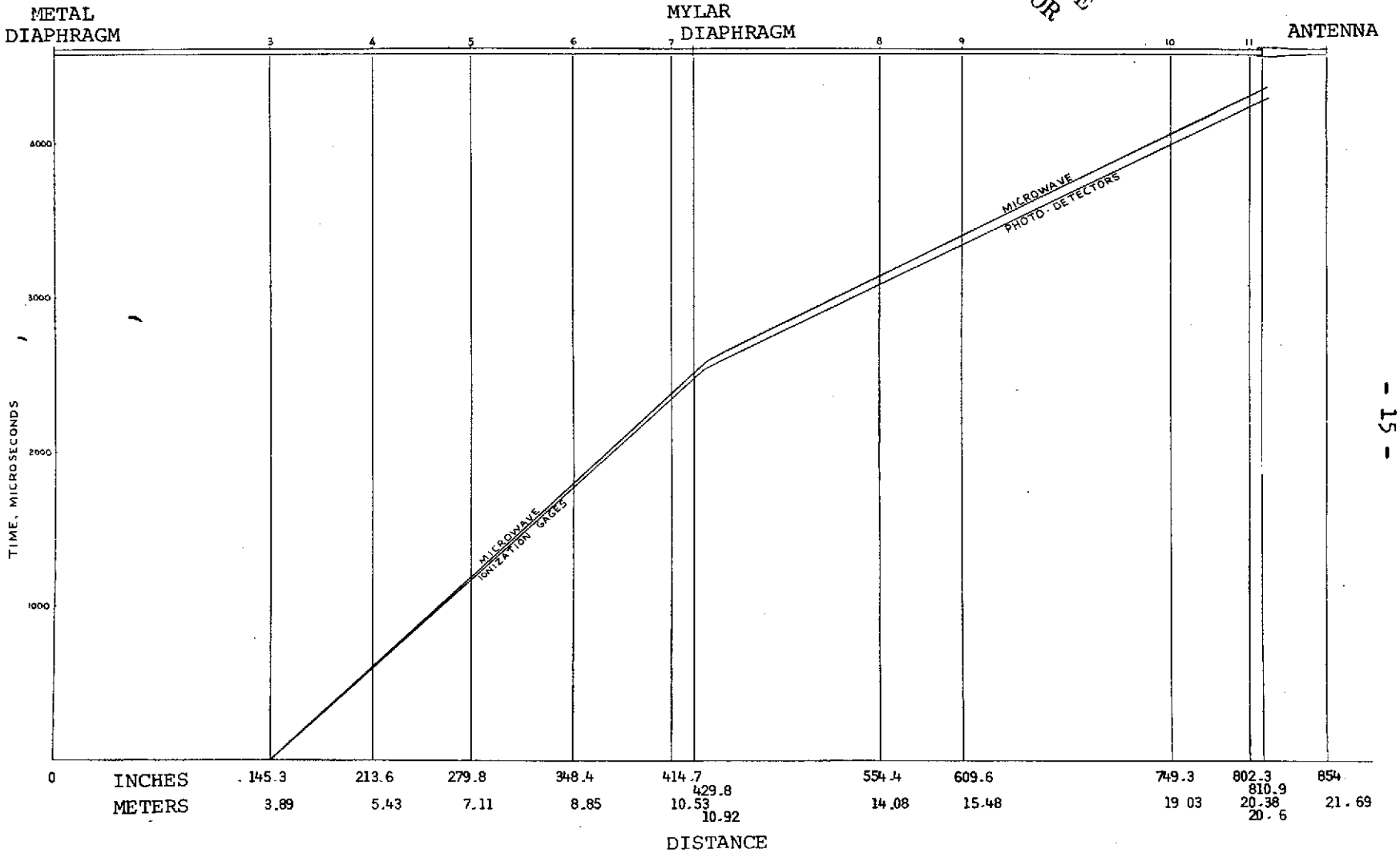

FIGURE 6. TIME OF REFLECTIVE SURFACE PASSING A POSITION VERSUS THIS POSITION.

Also plotted in figure 6 is the times at which the ionization and photo-detectors respond as a function of their position. Ionization detectors are located at stations 3, 4, 5, and 6 and photodetectors are located at stations 8, 9, and 10. A pressure transducer is located at the model to determine the time between shock and interface arrival. The ionization detectors should detect the interface between the shock and the test gas and the photo-detectors should detect the shock wave. The average velocity of the interface before the mylar diaphragm is 9508 ft/sec, less than 1% greater than the average velocity as determined by the microwave technique. Actually, although it cannot be seen on the plot, the microwave and ionization detector information appears to be in complete agreement for the first millisecond. After the mylar diaphragm ruptures the interferometer continues to track the test gas interface. The shock velocity as measured by the photo-detectors is 17,857 ft/sec, 1.5% greater than the interface velocity as measured by the microwave. The pressure transducer at the model detected the shock 50 microseconds before the arrival of the interface. The plots as shown in figure 6 indicates an arrival difference of 70 microseconds.

Also listed in table 2 are incremental velocities or average velocities over each $\lambda_g/2$ distance (5.096 inches) for the entire length of the expansion tube. Figure 7 is a plot of the incremental velocity versus distance from station 3. It can be noted that the test interface accelerates from 9,300 feet/second to 18,600 feet/second in a 20 inch distance.

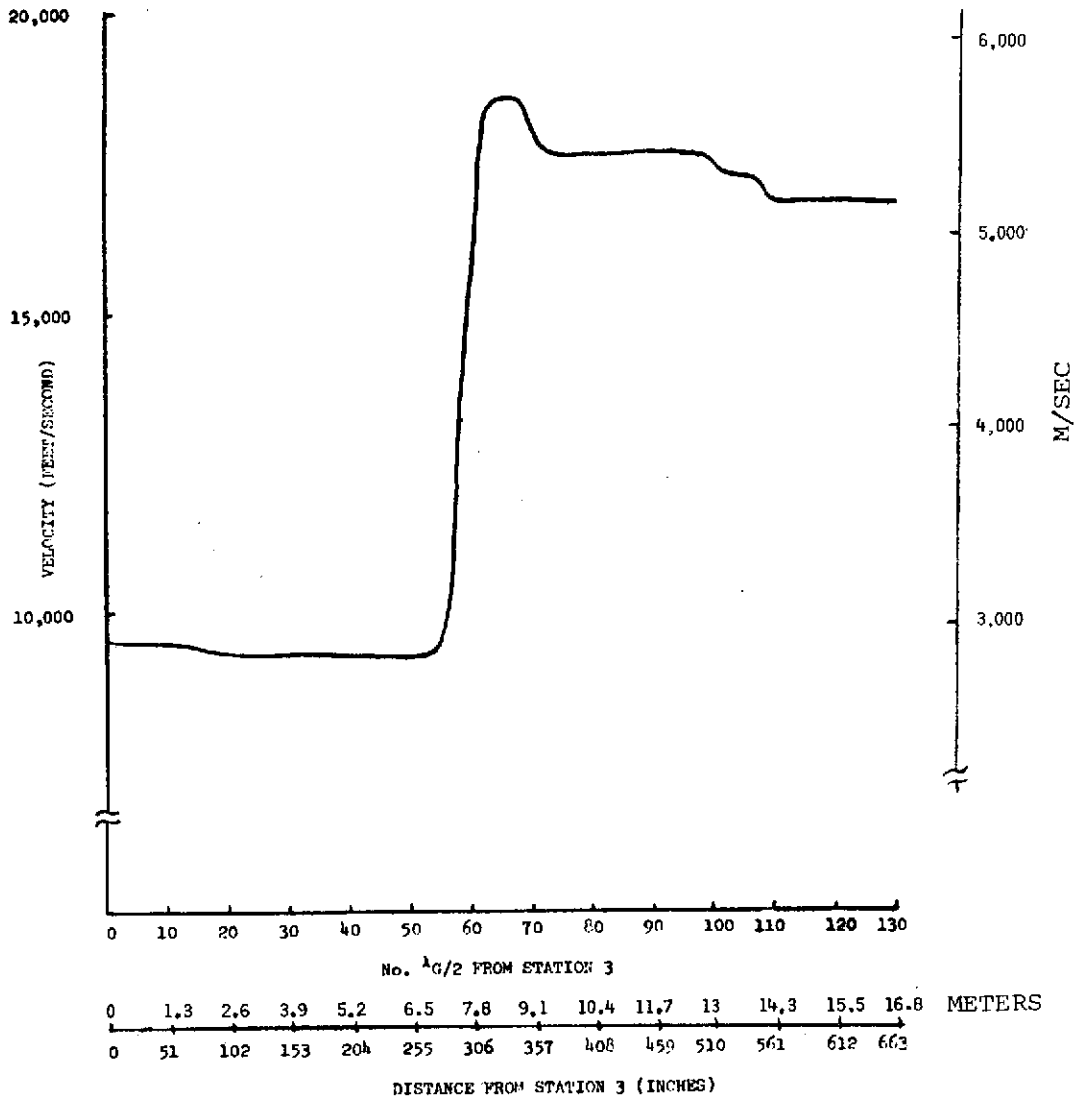

FIGURE 7. INCREMENTAL VELOCITY VERSUS REFLECTIVE SURFACE POSITION.

As stated before, run 1850 represents a typical run at the facility. However three parameters are frequently changed from run to run. They are (1) pressure of the test gas (2) pressure of the expansion tube and (3) mylar diaphragm thickness. Runs at test gas pressures of 100 mm (pressure expansion tube = .47 mm, 1/4 mil mylar) yield pre-mylar signals of about 10 millivolts and post-mylar signals of about 100 millivolts. Runs at expansion tube pressures of .215 mm, .095 mm, and .001 mm (other

parameters constant) yield pre-mylar signals of about 4 millivolts and post-mylar signals of 50 millivolts, 40 millivolts, and 20 millivolts all of which decayed to about 1/10 of this before the end of the expansion tube was reached. At the low pressures (0.001 mm) the system ceases to track the interface and the results are very incoherent. The effect of increasing the thickness of the mylar diaphragms is shown in figure 8.

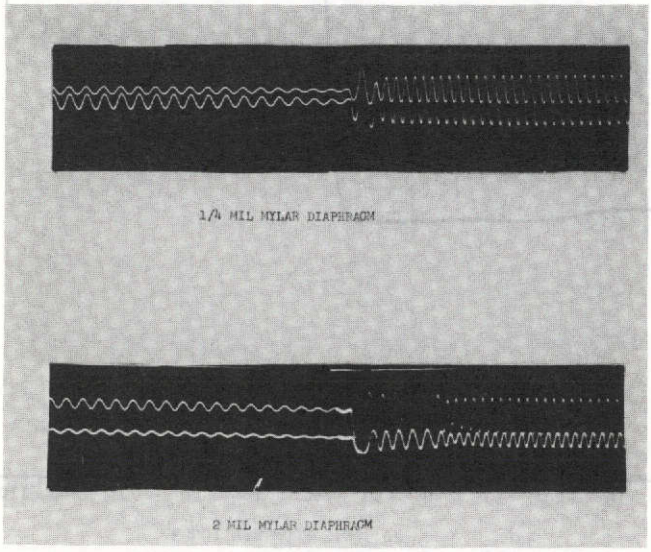

FIGURE 8. RUN RECORDS SHOWING EFFECT OF INCREASING DIAPHRAGM THICK.

DISCUSSION

The microwave interferometer as described in this report is capable of measuring average velocities of high-enthalpy, short duration gas flows in expansion tubes to an accuracy of better than 1% and incremental velocities (velocities over a $\lambda_g/2$ distance) can be measured to within 3%. Other reported systems have been used to track the shock wave or regions of high electron concentration immediately behind the shock wave; the tracking of the front interface is a unique development. [2,6]

The criteria which allows velocity measurements to be made using this method are (1) that the diameter of the tube and the frequency of operation are such that the fundamental mode may be excited and propagated down the tube and (2) that the electron concentration (Ne) of the moving surface is high enough so that the plasma frequency (f_p) is larger than the frequency of operation. For the operating frequency of 2.1758 kmc.[7]

$$f_p = 8.97 \times 10^3 \sqrt{Ne}$$

$$Ne = \left(\frac{2.1758 \times 10^9}{8.97 \times 10^3}\right)^2 = 5.88 \times 10^{10} \text{ electrons/cm}^3$$

Therefore the electron density of the reflecting surface must be greater than about 6×10^{10} cm^{-3} for reflections to occur. (Densities lower than this value will allow penetration of the plasma with only a shift in phase.)

The position time-history as presented in figure 6 contains errors which are difficult to determine. These errors are introduced by the change in the phase angle of the complex voltage reflection coefficient from its value before the mylar diaphragm to its value after the mylar diaphragm (which is constant for any run). A hint of this problem can be seen in figure 5. Between peaks 55 and 56 there is an apparent phase shift at the mylar diaphragm. It appears to be about a 90° phase shift between the signal just prior to the mylar diaphragm and the signal just after. This phase shift is evident in all runs although the value of the shift varies from run to run. Fortunately, the uncertainty in the position does not affect the average velocity or incremental velocity measurements.

Since the amplitude of the signal obtained by this method is not a quantitative measure of the reflection coefficient, only qualitative observations may be made. Assuming the reflective surface is air at some

temperature and pressure and using run 1850 as the sample, the temperature and pressure of the accelerated air is 3170°K and 36 psia respectively. The ratio ρ to ρ_o is 2.23×10^{-1}. The electron density and electron collision frequency can be found to be 6×10^{11} cm^{-3} and 2×10^{11} collisions/second.[8] For the purpose of illustration, calculations of the equations of a plane wave incident on an unbounded plasma slab of finite thickness were performed. Figures 9 and 10 are plots of power reflection coefficient versus electron concentration for various values of collision frequency. The frequency is 2.1758 kmc and a 2 centimeter reflecting slab is assumed. On figure 10, $Ne = 6 \times 10^{11}$ and $\nu = 2 \times 10^{11}$ yields a Γ_p of about .07 or a voltage reflection coefficient of .27. The 40 millivolt signal obtained amounted to about 45% of the signal obtained for a perfect reflector. Therefore before the mylar diaphragm the reflective surface may be considered as the test gas (air) at some pressure and temperature as a first approximation. However after the mylar, the temperature and pressure of the accelerated air are 1700°K and .3 psia respectively. ρ/ρ_o is 3.47×10^{-3}. The electron density is down to 10^4 cm^{-3} and $\nu = 10^9$ $second^{-1}$. Under these conditions nothing should be reflected from the air. The 100+ millivolt signal that results must be attributed to the increase in the instantaneous electron concentration behind the shock caused by the doubling of the velocity. Reported studies of ionization behind shock waves indicate that electron concentration increases with increasing mach number and decreases as ambient pressure decreases.[9] This could explain the fact that as the helium pressure was reduced the signal strength was also reduced.

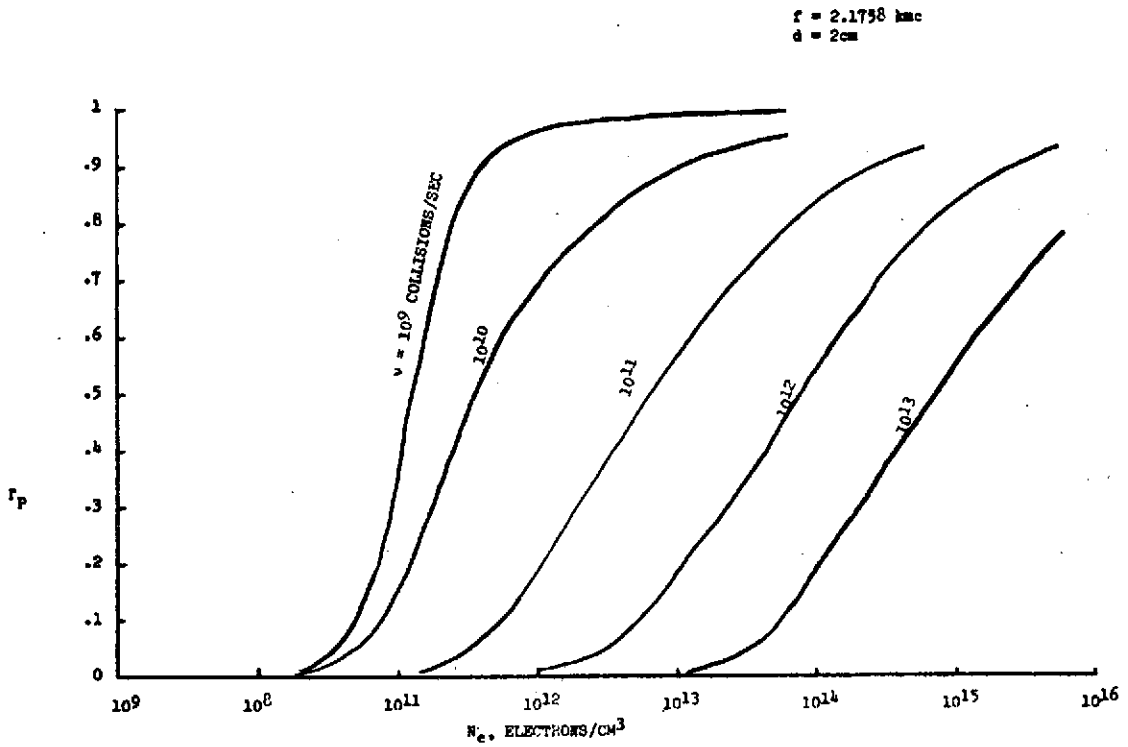

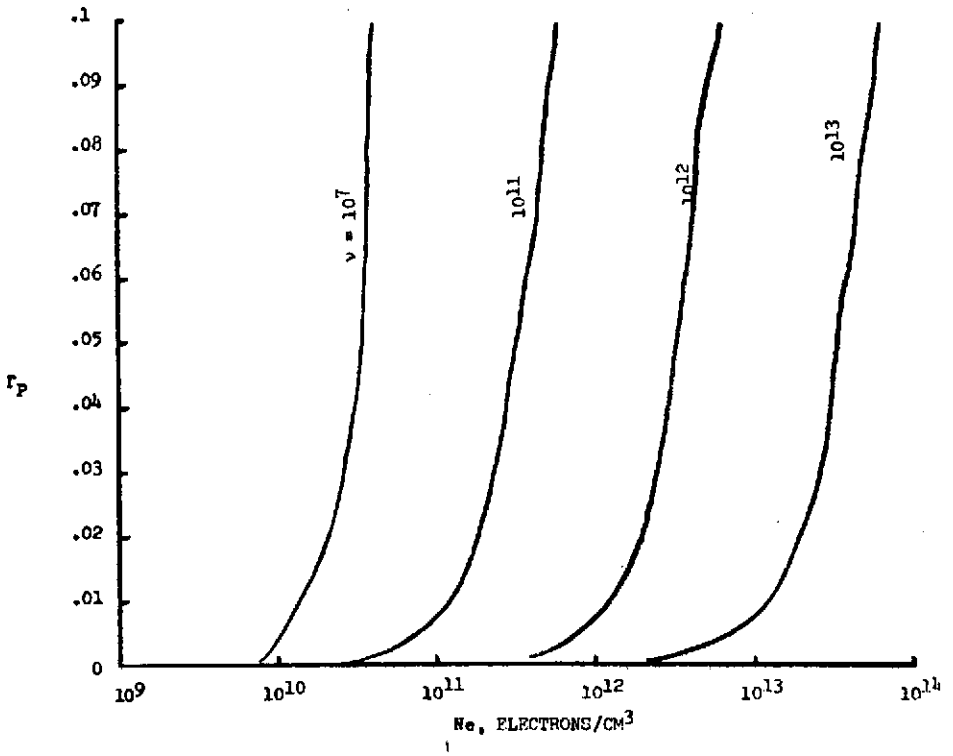

FIGURES 9 AND 10. POWER REFLECTION COEFFICIENT VERSUS ELECTRON CONCENTRATION.

The apparent loss of record is the last point of discussion. In all runs made the amount of record obtained between station 3 and the diaphragm was always shorter (always less than the 55.8 cycles calculated). Here again the key to this problem can be seen in figure 5. Note that the amplitude of the signal just prior to the diaphragm is about half the amplitude of the signal obtained at station 3. This decrease in amplitude indicates a change in the reflection coefficient caused by changes in either Ne or ν or both. Changes in Ne and ν also changes the complex reflection coefficient angle. (See figures 11 and 12).[10] Furthermore, to appear to lose record as is the case, the phase angle of the Γ_v should increase as Γ_v decreases. This is another way of saying that the conditions must by such that the operating point is to the left of the crossover point on the θ_{Γ_v} versus Ne curves. From the characteristics of the record prior to the mylar, Ne seems to be about 10^{11} cm^{-3} throughout the distance with a ν at station 3 of about 10^9 sec^{-1} and 10^{11} sec^{-1} just prior to the diaphragm.

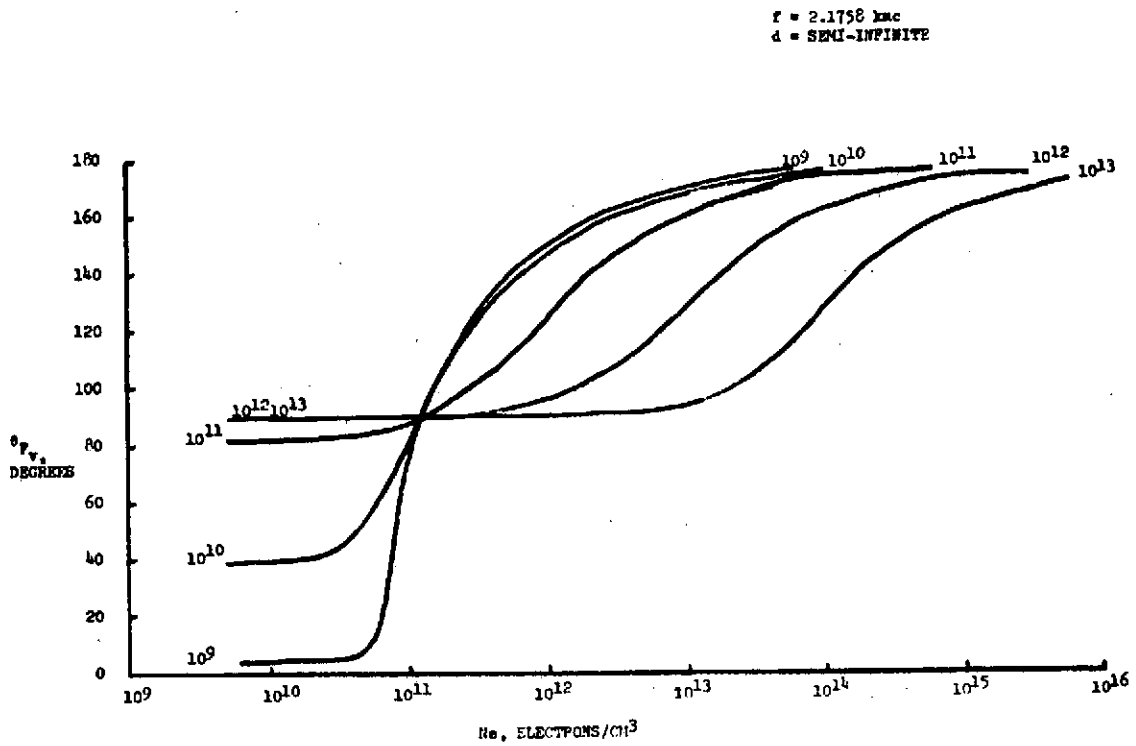

FIGURE 11. ANGLE OF VOLTAGE REFLECTION COEFFICIENT VERSUS ELECTRON CONCENTRATION.

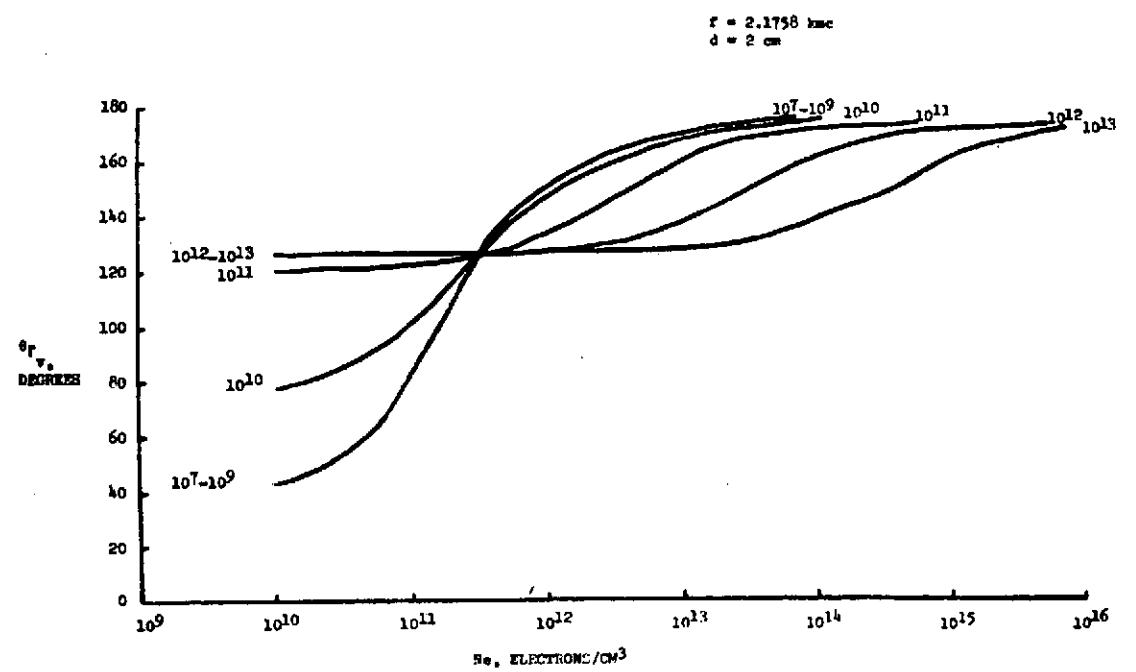

FIGURE 12. ANGLE OF VOLTAGE REFLECTION COEFFICIENT VERSUS ELECTRON CONCENTRATION.

CONCLUSION

The use of a microwave interferometer to measure incremental and average velocities of a gas front interface in an expansion tube (shock tube) facility has been demonstrated. The system has been used to measure velocities in excess of 20,000 ft/sec. Average velocity measurements were made to an accuracy of 1.0% which is comparable to existing techniques; incremental velocities over 5.0 inch distances were made accurate to within 3.0% which is unique with this system. The developed system has certain advantages over previously used techniques in that a continuous velocity record is obtained from measurements made at a single station. The measurement technique can be applied to any shock tube type gas front provided the electron concentration is high enough for reflection of the operating frequency signal.

ACKNOWLEDGEMENT

The author would like to express his appreciation to Jim J. Jones for his help in evaluating results and to the staff of his High-Pressure Shock-Tube for their cooperation in adapting this system to their facility, to William L. Grantham for his valuable advice and support in determining the microwave-plasma characteristics, and to John E. Jordan for his able assistance in operating the complete instrumentation system.

HBE CLR

REFERENCES

1. Terman, Frederick E.: Electronic and Radio Engineer, McGraw-Hill, 1955, Fourth Edition, pp. 156-157.

2. Schultz, D. L., et al: "Observations of Shock Wave Velocity in a Shock Tube with a Microwave Interferometer." Aeronautical Research Council, 20,901, 26th March, 1959.

3. Ramo and Whinnery: Fields and Waves in Modern Radio. Second Edition, Wiley, 1956, pp. 374-379.

4. Moreno, Theodore: Microwave Transmission Design Data, Dover, 1958, pp. 122-124.

5. Trimpi, R. L.: A Preliminary Study of a New Device for Producing High-Enthalpy, Short Duration Gas Flows, Second National Hypervelocity Techniques Symposium, 1963.

6. Rome Air Development Center Technical Documentary Report No. RADC-TDR-64-298, September 1964, Energy Transfer to Surfaces Through Ionized Shock Waves.

7. Drummond, J. E.: Plasma Physics, McGraw-Hill, 1961, pp. 264-267.

8. Bachynski et al: Proceedings of the IRE. Electromagnetic Properties of High-Temperature Air, March 1960, pp. 347-356.

9. Lin, S. C., et al: Rate of Ionization Behind Shock Waves in Air, Avco Everett Research Laboratory Report 105, September 1960.

10. Takeda and Tsukishima: Journal of the Physical Society of Japan. Microwave Study of Plasmas Produced by Electromagnetically Driven Shock Waves, Vol. 18, No. 3, March 1963.

TABLE 1. LIST OF COMPONENTS

SIGNAL GENERATOR	POLARAD MSG-1, .95-2.4 KMC, 1MW, 50Ω
ISOLATOR	SPERRY D44L15, COAXIAL, 1-2 KMC, 10DB MIN ISOLATION INS-LOSS 1DB MAX. VSWR 1.2 MAX
FREQ METER	SPERRY MICROLINE MODEL 124C
HYBRID	ALFORD AMCI TYPE 1102B-N 1.6 - 2.4 KMC
TUNING STUB	PRD 327, .95 - 5 KMC
VARIABLE ATTENUATOR	PRD 198, 1-4 KMC, 0-100DB
ADJUSTABLE SHORT	NARDA 372 NM, 2-12 KMC, 10W
TUNABLE DETECTOR MOUNT	SPERRY 34B1, .9-12.4 KMC, TYPE IN23-C DIODE
OSCILLOSCOPE	TEKTRONIX 555, P-16 PHOSPHOR, TYPE "D" PLUG IN
DRUM CAMERA	BECKMAN-WHITLEY 364, 35MM, .12 MM/ μS, 33-7/8" RECORD
EPUT METER	BECKMAN 7370, ACCURACY ± 1 COUNT

TABLE 2. TABULATION OF DISTANCE AND TIME BETWEEN PEAKS.

PEAK NUMBERS	DISTANCE (INCH)	TIME (μS)	CUMULATIVE TIME (μS)	INCREMENTAL VEL. (FT/SEC)
			0	
0-1	.233	55.9	55.9	
1-2	.185	44.4	100.3	9570.1
2-3	.185	44.4	144.7	9570.1
3-4	.185	44.4	189	9570.1
4-5	.185	44.4	233.4	9570.1
5-6	.187	44.8	278.3	9467.8
6-7	.185	44.4	322.6	9570.1
7-8	.187	44.8	367.5	9467.8
8-9	.185	44.4	411.9	9570.1
9-10	.187	44.8	456.7	9467.8
10-11	.187	44.8	501.6	9467.8
11-12	.187	44.8	546.5	9467.8
12-13	.187	44.8	591.3	9467.8
13-14	.187	44.8	636.2	9467.8
14-15	.19	45.6	681.7	9318.3
15-16	.19	45.6	727.3	9318.3
16-17	.187	44.8	772.2	9467.8
17-18	.19	45.6	817.8	9318.3
18-19	.19	45.6	863.3	9318.3
19-20	.19	45.6	908.9	9318.3
20-21	.19	45.6	954.5	9318.3
21-22	.19	44.8	1000.1	9318.3
22-23	.187	45.6	1044.9	9467.8
23-24	.19	45.6	1090.5	9318.3
24-25	.19	45.6	1136.1	9318.3
25-26	.19	45.6	1181.7	9318.3
26-27	.19	45.6	1227.2	9318.3
27-28	.19	45.6	1272.9	9318.3
28-29	.19	45.6	1318.4	9318.3
29-30	.19	45.6	1364	9318.3
30-31	.19	45.6	1409.5	9318.3
31-32	.19	45.6	1455.1	9318.3
32-33	.19	45.6	1500.7	9318.3
33-34	.192	46.1	1546.8	9221.2
34-35	.19	45.6	1592.3	9318.3
35-36	.19	45.6	1638	9318.3
36-37	.19	45.6	1683.5	9318.3
37-38	.19	45.6	1729.1	9318.3
38-39	.187	44.8	1774	9467.8
39-40	.192	46.1	1820	9221.2
40-41	.187	44.8	1864.8	9467.8
41-42	.192	46.1	1910.9	9221.2
42-43	.19	45.6	1956.5	9318.3
43-44	.19	45.6	2002.1	9318.3

PEAK NUMBERS	DISTANCE (INCH)	TIME (μS)	CUMULATIVE TIME (μS)	INCREMENTAL VEL. (FT/SEC)
44-45	.19	45.6	2047.6	9318.3
45-46	.187	44.8	2092.5	9467.8
46-47	.19	45.6	2138.1	9318.3
47-48	.19	45.6	2183.6	9318.3
48-49	.192	46.1	2229.7	9221.2
49-50	.19	45.6	2275.3	9318.3
50-51	.192	46.1	2321.3	9221.2
51-52	.192	46.1	2367.4	9221.2
52-53	.195	46.8	2414.2	9079.3
53-54	.19	45.6	2459.7	9318.3
54-55	.187	44.8	2504.6	9467.8
55-56	.165	39.6	2544.2	10730.1
56-57	.181	43.4	2587.6	9781.6
57-58	.125	30	2617.6	14163.8
58-59	.11	26.4	2644.0	16095.2
59-60	.11	26.4	2670.4	16095.2
60-61	.105	25.2	2695.8	16867.6
61-62	.1	24	2719.5	17704.7
62-63	.095	22.8	2742.3	18636.5
63-64	.095	22.8	2765.1	18636.5
64-65	.095	22.8	2787.9	18636.5
65-66	.095	22.8	2810.7	18636.5
66-67	.095	22.8	2833.5	18636.5
67-68	.095	22.8	2856.3	18636.5
68-69	.097	23.3	2879.5	18252.3
69-70	.098	23.5	2903.0	18066.
70-71	.1	24	2927.	17704.7
71-72	.1	24	2951.	17704.7
72-73	.1	24	2975.	17704.7
73-74	.1	24	2999.	17704.7
74-75	.1	24	3023.	17704.7
75-76	.1	24	3047.	17704.7
76-77	.1	24	3071.	17704.7
77-78	.1	24	3095.	17704.7
78-79	.1	24	3119.	17704.7
79-80	.1	24	3142.	17704.7
80-81	.1	24	3116.	17704.7
81-82	.1	24	3191.	17704.7
82-83	.1	24	3214.9	17704.7
83-84	.1	24	3238.9	17704.7
84-85	.1	24	3262.9	17704.7
85-86	.1	24	3286.9	17704.7
86-87	.1	24	3310.9	17704.7
87-88	.1	24	3334.8	17704.7
88-89	.1	24	3358.8	17704.7
89-90	.1	24	3382.8	17704.7
90-91	.1	24	3406.8	17704.7

PEAK NUMBERS	DISTANCE (INCH)	TIME (μS)	CUMULATIVE TIME (μS)	INCREMENTAL VEL. (FT/SEC)
91-92	.1	24	3430.8	17704.7
92-93	.1	24	3454.8	17704.7
93-94	.1	24	3478.8	17704.7
94-95	.1	24	3502.8	17704.7
95-96	.1	24	3526.8	17704.7
96-97	.1	24	3550.8	17704.7
97-98	.1	24	3574.8	17704.7
98-99	.102	24.5	3599.2	17357.5
99-100	.102	24.5	3623.7	17357.5
100-101	.1	24	3647.6	17704.7
101-102	.102	24.5	3672.1	17357.5
102-103	.102	24.5	3696.6	17357.5
103-104	.102	24.5	3721	17357.5
104-105	.1	24	3745	17704.7
105-106	.102	24.5	3769.5	17357.5
106-107	.102	24.5	3794	17357.5
107-108	.105	25.2	3819.2	16861.6
108-109	.105	25.2	3844.3	16861.6
109-110	.105	25.2	3869.5	16861.6
110-111	.105	25.2	3894.7	16861.6
111-112	.105	25.2	3920	16861.6
112-113	.105	25.2	3945.1	16861.6
113-114	.103	24.7	3969.8	17189
114-115	.104	24.9	3994.8	17023.7
115-116	.105	25.2	4020	16861.6
116-117	.105	25.2	4044.1	16861.6
117-118	.105	25.2	4070.3	16861.6
118-119	.103	24.7	4095	17189
119-120	.105	25.2	4120.2	16861.6
120-121	.105	25.2	4145.4	16861.6
121-122	.103	24.7	4170.1	17189.
122-123	.105	25.2	4195.3	16861.6
123-124	.105	25.2	4220.5	16861.6
124-125	.105	25.2	4245.7	16861.6
125-126	.105	25.2	4270.9	16861.6
126-127	.105	25.2	4296	16861.6
127-128	.105	25.2	4321.2	16861.6
128-129	.105	25.2	4346.4	16861.6
129-130	.105	25.2	4371.6	16861.6